On the disappearance of the *gem*-dimethyl effect: the base-catalysed cyclization of ethyl hydantoates †

Ergun Atay,[a] Iva B. Blagoeva,[a] Anthony J. Kirby[b] and Ivan G. Pojarlieff*[a]

[a] *Institute of Organic Chemistry, Bulgarian Academy of Sciences, ul. Acad. G. Bonchev block 9, Sofia 1113, Bulgaria*
[b] *University Chemical Laboratory, Cambridge, UK CB2 1EW*

Received (in Cambridge) 17th April 1998, Revised 31st July 1998, Accepted 3rd August 1998

Buffer catalysis and solvent kinetic isotope effects in the cyclization of methyl-substituted ethyl hydantoates with ω-*N*-methyl (MUE) and ω-*N*-phenyl groups (PUE) have been studied in an attempt to elucidate the changes in mechanism and eventual reversal of relative reactivities caused by increasing the number of substituent methyl groups (the *gem*-dimethyl effect). (Rate constants for the hydroxide-catalysed cyclization are actually reduced on going to the fully methylated compounds.) For catalysis by hydroxide inverse isotope effects are generally consistent with specific base-catalysed cyclization, but the cyclizations of the most heavily substituted compounds show normal isotope effects, indicating a change of mechanism. It is suggested that proton transfer to the ethoxide leaving group is slowed by steric hindrance, and becomes rate determining for the most substituted compounds **3**. Eclipsing strain in the tetrahedral intermediate may also be involved. The Brönsted plots for general base catalysis show distinctly different slopes of 0.2 for MUE and 0.6 for PUE, respectively. These are assigned to hydrogen bond preassociation and concerted catalysis mechanisms, of the attack of the ureido group nitrogen on the ester group. Rate constants for the reaction of the substrate anion would fall in the region of 10^{10} s^{-1} for esters **3** if the *gem*-dimethyl effect were fully expressed.

The carboxylation of biotin by hydrogen carbonate involves the reaction of a urea nitrogen with a carboxylate group, and the nucleophilic reactivity of ureas is of particular interest in this respect.[1] The introduction of methyl groups in positions 2 and 3 of hydantoic acids accelerates the cyclization to hydantoins up to 10^6-fold (a manifestation of the *gem*-dimethyl effect): an extreme case is the irreversible base-catalysed cyclization of the tetramethylhydantoate anion (Scheme 1).[2]

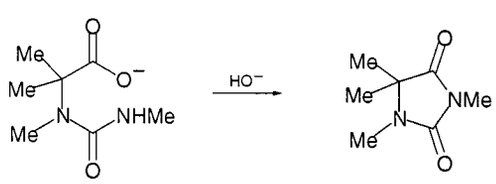

Scheme 1

Thus varying the number of methyl groups in the side-chain of a hydantoic acid derivative and the polarity of the substituent at the nucleophilic nitrogen provides model systems for the systematic study of various aspects of the reactivity of ureas. Central to the analysis is the partitioning of the tetrahedral intermediate, T. In reactions not involving cyclization varying the acyl substituent generally has little effect on the partitioning ratio, k_2/k_{-1} (Scheme 2), because both leaving groups are subject to similar effects. And the effects of structure on leaving group capabilities are readily predictable, except that steric effects involving the leaving group seem to have little effect on the partitioning ratio in the alkaline hydrolysis of secondary amides.[3] The *gem*-dimethyl effect superimposes a new element in cyclization reactions, favouring ring formation but slowing steps involved in ring opening. For example, the alkaline

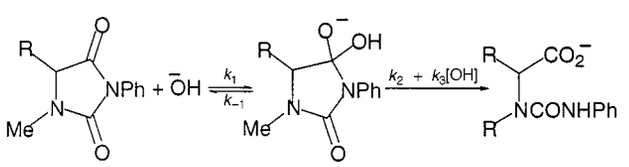

Scheme 2

hydrolysis of 1,5-dimethyl-3-phenylhydantoin (Scheme 2, R = Me) at low pH has k_2 rate-determining,[4] while 3-phenylhydantoin (R = H) is hydrolysed with rate-determining k_1.[5]

Typically in such reactions flexibility is lost progressively between the open chain and the final ring: the consequences for the partitioning of tetrahedral intermediates have been discussed recently in some detail.[6] But we had no convincing explanation for the apparent reversal of the *gem*-dimethyl effect observed in the OH^--catalysed ring closure of ω-phenylhydantoic esters.[7] This prompted this more detailed study of the cyclization of the two series of ethyl ω-methyl and ω-phenylhydantoates, **1**–**3**-MUE and PUE.

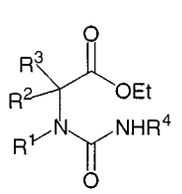

	R^1	R^2	R^3	R^4
1-MUE	Me	H	H	Me
2-MUE	Me	Me	H	Me
3-MUE	Me	Me	Me	Me
1-PUE	Me	H	H	Ph
2-PUE	Me	Me	H	Ph
3-PUE	Me	Me	Me	Ph

New buffer catalysis and kinetic solvent isotope effect data allow a more definitive explanation of the change in the partitioning ratio, to rate determining breakdown of the tetrahedral intermediate in the most highly substituted compounds.

Experimental

Materials

Inorganic reagents and buffer components were of analytical

† Supplementary material is available for this paper (SUPPL. NO. 57422, 8 pp.) For details of the Supplementary Publications Scheme see '*Instructions for Authors*', *J. Chem. Soc.*, *Perkin Trans. 2* available *via* the RSC web page (http://www/rsc/org/authors).

Table 1 Rate constants for H^+, OH^- and H_2O catalysed ring closure of ethyl hydantoates

Compound	k_H/dm^3 mol^{-1} s^{-1}	k_w/s^{-1}	k_{OH}/dm^3 mol^{-1} s^{-1}
1-MUE	$(7.41 \times 10^{-4})^a$		44.1 ± 0.9^b
2-MUE[c]	$(2.56 \pm 0.26) \times 10^{-2}$	$(7.41 \pm 1.30) \times 10^{-6}$	447 ± 63
3-MUE	2.00 ± 0.07	$(4.20 \pm 0.19) \times 10^{-4}$	1045 ± 53
1-PUE	$(1.03 \pm 0.14) \times 10^{-4}$		$(8.43 \pm 0.55) \times 10^{4e}$
2-PUE	$(3.25 \pm 0.13) \times 10^{-3}$	$(1.43 \pm 0.15) \times 10^{-5d}$	$(9.51 \pm 0.34) \times 10^5$
3-PUE	$(1.28 \pm 0.02) \times 10^{-1}$	$(1.68 \pm 0.15) \times 10^{-5d}$	$(2.17 \pm 0.05) \times 10^5$

[a] Observed rate in 1 M HCl. [b] From several experiments in dilute carbonate buffers; ref. 14 reports 24 dm^3 mol^{-1} s^{-1}. [c] Data from ref. 9. [d] Values less precise because of indistinct plateaux in the rate profile. [e] 1.2×10^5 dm^3 mol^{-1} s^{-1} according to ref. 14.

grade and used without further purification. Potassium hydroxide and buffer solutions were prepared with CO_2-free distilled water. D_2O and DCl (20 wt% in D_2O), 99 atom% D were from Aldrich.

The preparation of ethyl hydantoates **1**-MUE and (**1**–**3**)-PUE was described previously.[8] All stock solutions of the substituted ethyl 5-phenylhydantoates were prepared in dry THF.

3-MUE was prepared *in situ* as described for **2**-MUE.[9] The ester cyclized readily in the presence of traces of moisture in the THF solution, so stock solutions were prepared before each series of kinetic runs by injecting methyl isocyanate (10.5 μl, 0.165 mmol) through a septum into 1 ml dry THF containing ethyl 2-amino-2-methylpropionate (0.15 mmol). Samples were withdrawn in the same way. Stock solutions were stored frozen between kinetic runs and were kept for no more than 6 hours.

The hydantoins used in the product analysis were prepared by known procedures and their mp agreed with literature values: 1,3-dimethylhydantoin,[10] 1,3,5,5-tetramethylhydantoin,[2] 1-methyl-3-phenylhydantoin,[11] 1,5-dimethyl-3-phenylhydantoin,[4] 3-phenyl-1,5,5-trimethylhydantoin.[12]

Product analysis

The ethyl hydantoates cyclized quantitatively to the corresponding hydantoins. The end-points for the kinetic runs were identical within experimental error with the absorbances of solutions of the authentic hydantoins.

For **2**-PUE and **3**-PUE the reaction products resulting from base-catalysed ring closure were isolated as follows. A solution of **2**-PUE or **3**-PUE (0.044 mmol in 0.5 ml THF) was added to 28 ml phosphate buffer, pH 6.5, and the reaction mixture kept for 35 min at room temperature. The solution was then evaporated to dryness and the residue extracted with 3×10 ml CH_2Cl_2. The combined organic layers were dried over $MgSO_4$ and evaporated to give hydantoin (78–80%). Products were identical (mp, NMR) with samples of the respective hydantoins prepared by literature methods.

Kinetic measurements

Rate constants were determined at 25.0 ± 0.01 °C under pseudo-first-order conditions in the thermostatted cell compartment of a Unicam SP-800 spectrophotometer. The rates for cyclization of the substituted esters were followed by monitoring the changes of the absorbances at wavelengths in the 240–247 nm range. In the case of substrates with ω-phenylureido groups the decrease of the absorbance due to phenylhydantoic ester was monitored, while for ω-methylureido compounds only the increase of absorbance due to the hydantoin ring formation could be followed. Reactions were initiated by injecting 20–50 μl of $1–2 \times 10^{-2}$ M stock solutions of (**1**–**3**)-PUE and 25–30 μl of 2×10^{-1} M stock solutions of (**1**–**3**)-MUE into 2.7 ml preheated buffer solution. Ionic strength was maintained constant (1 M) with KCl. Measurements of pH-values and calculations of first-order rate constants (k_{obs}) were as previously described.[4] Good first-order linear plots ($r > 0.999$) were obtained over three half-lives and k_{obs}-values were reproducible to within ±3%.

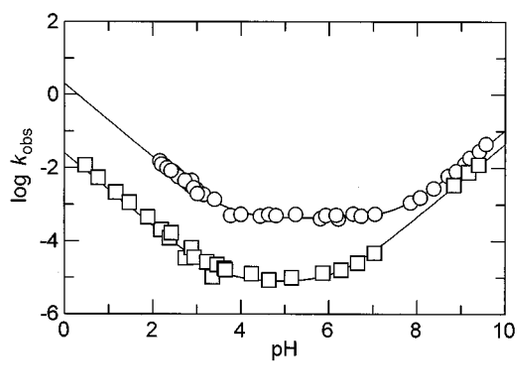

Fig. 1 Rate profiles for the cyclization of ethyl 5-methylhydantoates **2**-MUE (○) and **3**-MUE (□); lines drawn are calculated from eqn. (1) using parameters from Table 1.

Kinetic solvent isotope effects

The determination of KSIE for the hydroxide-catalysed ring closure of the substrates was complicated by the occurrence of buffer catalysis. The procedure adopted for all six ethyl hydantoates consisted of measuring k_{obs}-values at three buffer concentrations in the range 0.01–0.05, at pH values where the reaction is clearly first order in OH^-: in phosphate buffer (20 and 30% free base) with **1**–**3**-PUE and in carbonate (10 and 30% free base) with **1**–**3**-MUE. k_{OH}-values were obtained by extrapolating to zero buffer concentration. For reactions where k_{obs} changed with buffer concentration by less than 6% the mean value was taken, and divided by the activity of HO^- or DO^- to obtain k_{OH} or k_{OD}. pD-values were obtained by adding 0.4 to the pH-meter readings and the a_{OD}-values calculated using $pK_w = 14.86$.[13]

Results

Rate constants for catalysis by $[H^+]$, $[OH^-]$ and water were obtained by fitting the rate profiles to eqn. (1). The pseudo-first-

$$k_{obs} = k_H a_H + k_{OH} a_{OH} + k_w \quad (1)$$

order rate constants, k_{obs}, are values extrapolated to zero buffer concentration. The activities of H^+ and OH^- were obtained from the pH-values measured in the most dilute buffer in the series of a given buffer ratio. For runs in HCl the concentrations of the acid at ionic strength of 1 M (KCl) were converted to activities using an activity coefficient of 0.851.[7] For the slower reactions of **1**-PUE and **1**-MUE only limited numbers of data points were obtained, for evaluation of the *gem*-dimethyl effect. The rate constants are summarized in Table 1 and the fits to experimental data shown on Figs. 1 and 2.

Second-order rate constants for catalysis by buffer components were obtained by fitting the data to eqn. (2). The

$$k_{obs} = k_{HA}[HA] + k_B[B] + k_H a_H + k_{OH} a_{OH} + k_w \quad (2)$$

preferred procedure was to treat k_H, k_{OH} and k_w as known constants using the values from Table 1, omitting as appropriate

Table 2 Buffer catalysis data for the cyclization of ethyl 2,2,3,5-tetramethylhydantoate (**3**-MUE) at 25 °C and ionic strength 1.0 M

Buffer acid	pK_{AH} [a,b]	Conc. range/mol dm^{-3}	Runs	% Base	$k_{AH}/10^{-4}$ dm^3 mol^{-1} s^{-1} [b]	$k_B/10^{-4}$ dm^3 mol^{-1} s^{-1} [b]
H_3O^+	−1.74				20000 ± 700	4.20 ± 0.19 [c]
	(−1.26)				(6660)	
H_3PO_4	1.78	0.006–0.7	5	60	3460 ± 130	360 ± 39 [d]
	(2.26)	0.08–0.7	5	70	(1150)	
		0.0056–0.7	5	80		
		0.1–1	5	90		
$H_3N^+CH_2CO_2H$	2.45	0.1–0.5	4	40	768 ± 11	45.1 ± 7.1
		0.1–0.5	4	60		
		0.1–0.5	4	70		
		0.1–0.5	4	80		
HCO_2H	3.57	0.1–0.5	5	20	396 ± 61	81.2 ± 6.4
		0.1–0.5	5	40		
		0.1–0.35	4	60		
		0.1–0.5	5	80		
CH_3CO_2H	4.62	0.1–0.5	4	20	142 ± 0.01	117 ± 1
		0.1–0.5	4	40		
		0.1–0.5	4	50		
		0.1–0.5	4	60		
		0.1–0.5	4	80		
$(CH_3)AsO_2H$	6.19	0.05–0.3	4	30	78.6 ± 3.3	556 ± 3
		0.05–0.3	4	50		
		0.05–0.3	4	70		
$H_2PO_4^-$	6.48	0.016–0.7	7	20	352 ± 7	815 ± 10
		0.016–0.6	8	30	(176)	(407)
		0.016–0.5	8	50		
		0.016–0.4	8	60		
		0.016–0.4	8	75		
HCO_3^-	9.69	0.04–0.1	4	10		2480 ± 140
		0.04–0.1	4	20		1240
		0.04–0.1	4	30		
		0.04–0.1	4	40		
H_2O	15.74					(1.045 ± 0.050) × 10^7

[a] pK_{AH}-values taken from ref. 4. [b] Statistically corrected values in parentheses. [c] First-order rate constant. [d] Not included in the Brönsted correlation.

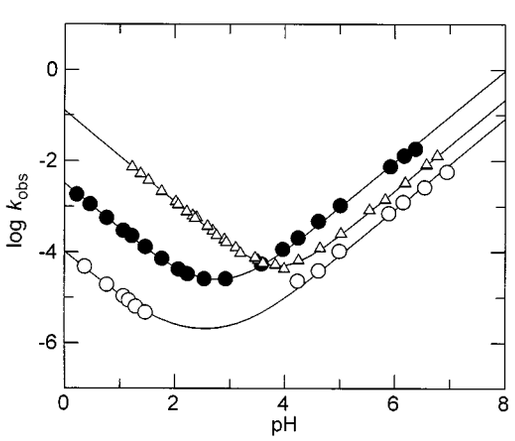

Fig. 2 Rate profiles for the cyclization of ethyl 5-phenylhydantoates **1**-PUE (○), **2**-PUE (●), and **3**-PUE (△). Lines drawn are calculated from eqn. (1) using parameters from Table 1. (Reproduced from ref. 7 with permission of the Royal Society of Chemistry.)

terms that do not contribute significantly. These results are summarized in Tables 2–5, and full details are given as supplementary data.

As observed previously[9] with **2**-MUE, the rates of cyclization of **3**-MUE in TRIS and carbonate increased with buffer concentration (up to 0.10 dm^3 mol^{-1}) by only *ca.* 20%. Nevertheless a good fit for the carbonate data was obtained with the equation containing the terms for carbonate and OH^- catalysis only. On the other hand, an extended set of 19 data points in TRIS buffers (0.04 to 0.50 dm^3 mol^{-1}) gave no stable solution for k_B and k_{AH}. Similar complications with buffers containing free amines have been observed previously in the cyclization of hydantoic acids and esters and were attributed to inhibition by the free amine.[2,9] That general base catalysis is possible at these pH-values is demonstrated by experiments using sodium cacodylate in 0.05 M TRIS as carrier buffer at pH 8.4. k_{obs}-values were more than tripled in the presence of 0.32 M cacodylate. The k_B found (5.49 ± 0.40 × 10^{-2} dm^3 mol^{-1} s^{-1}) is in good agreement with the k_B-value found in cacodylate buffers (Table 2).

Though only similarly weak buffer catalysis was observed with **1**-PUE and **2**-PUE, the cyclization of **3**-PUE showed strong buffer catalysis. Formally this might be because buffer catalysis for the former compounds is superimposed on a relatively greater background rate. In our preliminary communication[7] we considered buffer catalysis not to be significant for the reactions of **1** and **2**-PUE. However, further measurements using more buffers and detailed regression analysis according to eqn. (2) gave what we consider to be meaningful values of k_B (k_{AH} were too small to be estimated accurately). Thus catalysis of the ring closure of **2**-PUE by KH_2PO_4 in a glycine carrier buffer of pH *ca.* 3 is attributed to the anion acting as a general base. In the case of **3**-PUE both acid and base catalysis are clearly expressed (the former in the more acidic buffers, up to and including acetic acid).

In $H_2PO_4^-/HPO_4^{2-}$ buffers plots of the second-order constants for buffer catalysis, k_{buffer}, against fraction base for **1**-PUE and **3**-PUE were curved, the slope rising sharply at higher fractions of free base (**2**-PUE was studied only at lower % free base) (Fig. 3a). The observed rate constants were well-fitted (Fig. 3b) by including the cross-term, eqn. (3):

$$k_{obs} = k_B[B] + k_{BOH}[B][OH] + k_{OH}[OH] + k_w \quad (3)$$

The constant k_{BOH} is best explained in terms of catalysis by PO_4^{3-}: its contribution becomes significant at higher pH and base concentrations because of the higher Brönsted β with the PUE series (*v.i.*). Since the reaction $HPO_4^{2-} + OH^- \rightleftharpoons PO_4^{3-} + H_2O$; gives eqn. (4) then the rate coefficient for catalysis by the phosphate trianion is given by eqn. (5).

Table 3 Buffer catalysis data for the cyclization of ethyl 3-methyl-5-phenylhydantoate (**1**-PUE) at 25 °C and ionic strength 1.0 M

Buffer acid	pK_{AH} [a,b]	Conc. range/mol dm^{-3} [c]	% Base	$k_{AH}/10^{-4}$ dm^3 mol^{-1} s^{-1} [b]	$k_B/10^{-4}$ dm^3 mol^{-1} s^{-1} [b]
H_3O^+	−1.74			1.03 ± 0.14	
	(−1.26)			(0.343)	
CH_3CO_2H	4.62	0.1–0.5	30		1.02 ± 0.14
		0.1–0.5	50		
		0.1–0.5	70		
$H_2PO_4^-$	6.48	0.14–0.7	20		32.4 ± 18
		0.12–0.6	30		(16.2)
		0.1–0.5	50		
		0.1–0.4	70		
HPO_4^{2-}	12.32 [d]				(240 ± 17) × 10^4
	(11.84)				(80) × 10^4
H_2O	15.74				(8.43) ± 0.54) × 10^8
	(16.04)				

[a] pK_{AH}-values taken from ref. 4. [b] Statistically corrected values in parentheses. [c] Four runs were carried out within each concentration range. [d] Calculated from $k_{BOH} = (1.15 \pm 0.08) \times 10^5$.

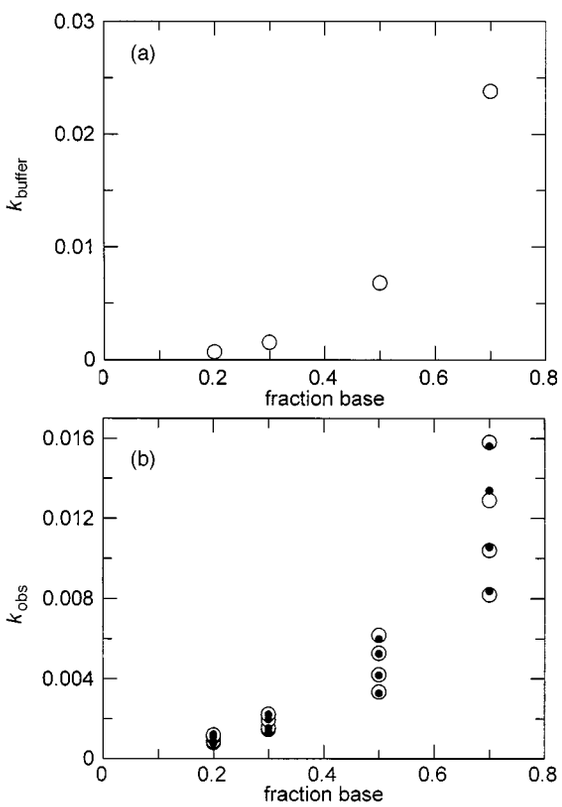

Fig. 3a Plot of k_{buffer} against fraction base for **1**-PUE in $H_2PO_4^-$/HPO_4^{2-} buffers. **3b**. Data for **1**-PUE in $H_2PO_4^-$/HPO_4^{2-} buffers; experimental points (○), calculated by means of eqn. (3) and parameters of Table 4 (●) presented as a function of fraction base only.

$$\frac{K_{HPO_4^{2-}}}{K_w} = \frac{[PO_4^{3-}]}{[HPO_4^{2-}][OH^-]} \quad (4)$$

$$k_{PO_4^{3-}} = k_{BOH}\frac{K_w}{K_{HPO_4^{2-}}} \quad (5)$$

The catalytic constant $k_{PO_4^{3-}}$ obtained for **3**-PUE fits the Brönsted plot (Fig. 5) well. Brönsted plots for the cyclization of the ureido esters are shown as Figs. 4–6. Kinetic solvent isotope effects k_{OH}/k_{OD} (KSIE, Table 6) were determined from runs in alkaline buffers as described in the Experimental section.

Both general acid and general base catalysis were observed with **3**-MUE and **3**-PUE, as shown previously for **2**-MUE. The rate constants k_B obtained for the weakest base, $H_2PO_4^-$ (also for $NCCH_2CO_2^-$ for **3**-PUE), showed large positive deviations from the line defined by the remaining bases, suggesting that the

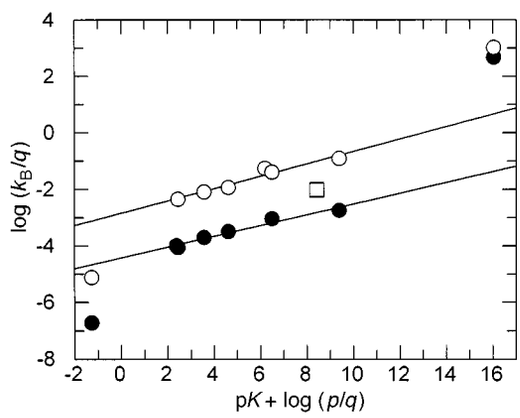

Fig. 4 Brönsted plots for GBC of the cyclization of ethyl 5-methylhydantoates **2**-MUE (●), data from ref. 9, **3**-MUE (○). The square is the deviant point for catalysis in TRIS with **3**-MUE. The lines drawn exclude the points for water and OH^-.

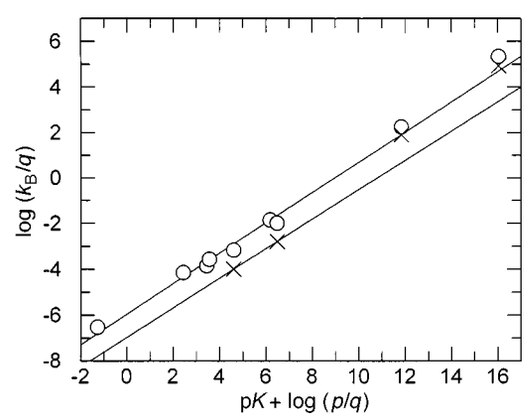

Fig. 5 Brönsted plot for GBC of the cyclization of ethyl 5-phenylhydantoates **3**-PUE (○) and **1**-PUE (×). The line drawn for **3**-PUE excludes the point for OH^-. The line for **1**-PUE is drawn through the two points for acetate and HPO_4^{2-} catalysis.

major contribution comes from the kinetically equivalent general acid catalysis by the phosphate monoanion. With **2**-PUE the second point in the plot of Fig. 6, for $H_2PO_4^-$, also shows a positive though small deviation.

Constructing the Brönsted plots in the case of **2**- and **3**-MUE presents two possibilities, as discussed previously [9] in the case of **2**-MUE. The inverse isotope effect is consistent with specific catalysis for the OH^- reaction of **2**-MUE, and so compatible with a positive deviation from the Brönsted plot for general base catalysis: the deviation (based on the low β) is some 4 log

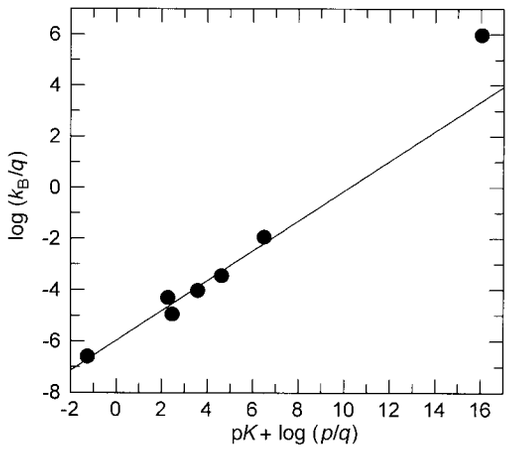

Fig. 6 Brönsted plot for GBC of the cyclization of ethyl 5-phenylhydantoate **2**-PUE. The line drawn excludes the point for OH^--catalysis.

units. The OH^- reaction of **3**-MUE shows a normal isotope effect ($k_H/k_D = 2.2$) and the deviation is reduced to 2 log units: as discussed below we believe this reaction differs from that catalysed by the less basic anions. The situation with **2**- and **3**-PUE is similar; although because of the larger Brönsted β the positive deviations of the OH^--points are smaller. While the points for water catalysis deviate strongly in the case of **2**- and **3**-MUE, they fall on the Brönsted line in the case of **2**- and **3**-PUE. (These k_w-values are less accurate because of the lack of clear plateaux for the water reaction in the rate profiles. However, omission of the water points for **2**- and **3**-PUE does not change the slopes significantly.) Linear regression analysis yields the following β-values.

Compound	β	r
2-MUE	0.19	0.982
3-MUE	0.22	0.973
2-PUE	0.58	0.982
3-PUE	0.66	0.995

Discussion

The main object of the present study was to rationalize the effects of steric strain on the mechanism of the base-catalysed cyclization of hydantoic esters which lead to the change of mechanism and apparent reversal of the *gem*-dimethyl effect with **3**-PUE. As shown by the pH-rate profiles of Figs. 1 and 2, and quantitatively by the data for relative rates of the various reactions in Table 7, the acceleration in k_{OH} due to the *gem*-dimethyl effect is much reduced also for the ω-*N*-methyl esters when compared to the accelerations observed in the acid-catalysed reaction, and the same factors are likely to be operating.

Specific base catalysis

The mechanism of the base-catalysed ring closure of hydantoic acid esters was discussed by Sterba and co-workers in their comprehensive kinetic study.[14] These authors assumed the formation of the C–N bond to be rate determining since the less basic ethoxy group should leave more readily from the tetrahedral intermediate than ureide nitrogen. They do not report general base catalysis, in contrast to the cyclization of thioureidoesters.

Rate-determining formation of the tetrahedral intermediate in the cyclization of typical ω-*N*-methyl esters is strongly supported by studies of the related reverse reaction, the alkaline hydrolysis of hydantoins: rate-determining cleavage of the C–N bond at lower pH is reliably indicated by a change in rate determining step and by the appearance of terms second order in OH^-.[15] The kinetics yielded an estimated partitioning ratio for hydantoin itself according to which OH^- leaves at least 100 times more readily than ureide anion. With *N*-aryl derivatives, however, the rate was only first order in OH^-.[5] The acidity of the phenylureido group is some three orders of magnitude greater than that of the methylureido group,[8] and thus similar to that of ethanol. This and other evidence led to the conclusion that hydrolysis proceeds by rate-determining C–O bond formation (equivalent to rate determining loss of ethoxide in ester cyclization). The *gem*-dimethyl effect facilitates cyclization but hinders ring opening, effectively making ureide a poorer leaving group. A result is the switch to rate-determining C–N cleavage observed in the alkaline hydrolysis of the hydantoin derived from **2**-PUE.

With this background we expect the specific base-catalysed cyclizations of compounds **1** and **2** to involve rate-determining formation of the tetrahedral intermediate. Scheme 3 shows the

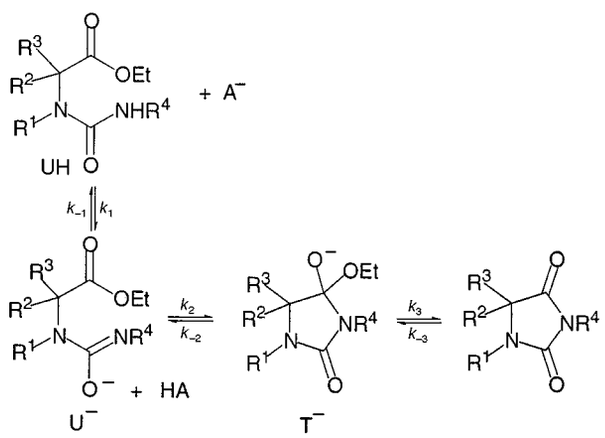

Scheme 3

mechanism for specific base catalysis, where k_2 is rate determining. The rate constants k_1 for deprotonation of NH by OH^- (recently reported as hydrogen exchange rates[8]) are some two orders of magnitude greater than k_{OH} for cyclization for all the compounds discussed in this work (Table 1). Thus the formation of U^- from UH is a preliminary equilibrium, consistent with the inverse isotope effect observed for the reactions of compounds **1** and **2**.

Table 8 shows values for k_{U^-}, the rate constant for the cyclization of U^- (Scheme 3) calculated from equilibrium concentrations of U^- (based on the pK-values recently determined for these esters[8]). The rate ratios for compounds **1** and **2** are similar to those shown below (Table 7) for the overall hydroxide-catalysed reactions, consistent with the rapid pre-equilibrium formation of U^-. However, if the *gem*-dimethyl effect were fully expressed for compounds **3** (*i.e.* the rates increased *ca.* 30-fold compared with compounds **2** as they do in acid), k_{U^-} would be in the region of 10^{10} s^{-1}. In fact the observed rate constants for the cyclization of the fully methylated anions $\mathbf{3}U^-$ are smaller than for **2**, and the reaction shows a normal solvent kinetic isotope effect of around 2. Evidently a different step, involving proton transfer, has become rate determining.

Of a total of four proton transfers which might be involved the deprotonation of the ureido-group (k_1) is too fast to be rate determining, as discussed above; and we rule out proton transfer to and from the O^- of T^- on the basis of the second-order term observed in the alkaline hydrolysis of hydantoins. There remains slow proton transfer to departing ethoxide (k_3 of Scheme 3); *i.e.* general acid catalysis by solvent water of the breakdown of T^-.

A mechanism of this sort was suggested in Gravitz and Jencks' detailed study[16] of the GBC breakdown *via* T^- of stable tetrahedral intermediates containing an alkoxy and amido group (though in their example the alkoxy group was intramolecular and the amine exocyclic). These authors doubted its

Table 4 Buffer catalysis data for the cyclization of ethyl 2,3-dimethyl-5-phenylhydantoate (**2**-PUE) at 25 °C and ionic strength 1.0 M

Buffer acid	pK_{AH} [a,b]	Conc. range/mol dm^{-3} [c]	% Base	$k_B/10^{-4}$ dm^3 mol^{-1} s^{-1} [b]
H_3O^+	−1.74			0.142 ± 0.015 [d]
	(−1.26)			
H_3PO_4	1.78	0.1–0.8	100	0.501 ± 0.029 [e]
	(2.26)			
$H_3N^+CH_2CO_2H$	2.45	0.1–1	30	0.113 ± 0.023
		0.1–1	50	
		0.1–1	70	
HCO_2H	3.57	0.1–0.5	50	0.939 ± 0.077
		0.1–0.5	70	
CH_3CO_2H	4.62	0.1–0.5	30	3.53 ± 0.39
		0.1–0.5	50	
		0.1–0.5	70	
$H_2PO_4^-$	6.48	0.14–0.7	20	230 ± 19
		0.072–0.6	30	(115)
		0.1–0.5	40	
H_2O	15.74			(9.51 ± 0.34) × 10^9

[a] pK_{AH}-values taken from ref. 4. [b] Statistically corrected values in parentheses. [c] Four runs were carried out within each concentration range. [d] First-order rate constant. [e] In carrier buffer 0.1 M acid glycine 70% base.

Table 5 Buffer catalysis data for the cyclization of ethyl 2,2,3-trimethyl-5-phenylhydantoate (**3**-PUE) at 25 °C and ionic strength 1.0 M

Buffer acid	pK_{AH} [a,b]	Conc. range/mol dm^{-3} [c]	% Base	$k_{AH}/10^{-4}$ dm^3 mol^{-1} s^{-1} [b]	$k_B/10^{-4}$ dm^3 mol^{-1} s^{-1} [b]
H_3O^+	−1.74			(1.27 ± 0.02) × 10^3	0.168 ± 0.015 [d]
	(−1.26)			(423)	
H_3PO_4	1.78	0.1–1	50	19.0 ± 0.5	5.50 ± 0.26
	(2.26)	0.1–1	70	(6.33)	
		0.1–1	90		
$NCCH_2CO_2H$	2.38	0.1–0.5	30	4.78 ± 0.86	2.71 ± 0.86
		0.1–0.5	50		
		0.1–0.5	70		
$H_3N^+CH_2CO_2H$	2.45	0.1–0.5	50	4.97 ± 0.46	0.706 ± 0.22
		0.1–0.5	70		
		0.1–0.5	90		
$CH_3OCH_2CO_2H$	3.46	0.1–0.5	30	3.33 ± 0.11	1.40 ± 0.11
		0.1–0.5	50		
		0.1–0.5	70		
HCO_2H	3.57	0.1–0.5	30	2.90 ± 0.11	2.68 ± 1.06
		0.1–0.5	50		
		0.1–0.5	70		
CH_3CO_2H	4.62	0.1–0.5	30	2.27 ± 0.14	6.77 ± 0.14
		0.1–0.5	50		
		0.1–0.5	70		
$(CH_3)AsO_2H$	6.19	0.05–0.3	30	Uncertain	140 ± 5
		0.05–0.3	50		
		0.05–0.3	70		
$H_2PO_4^-$	6.48	0.2–0.8	10		206 ± 5
		0.1–0.6	30		(103)
		0.1–0.5	50		
		0.1–0.45	60		
HPO_4^{2-}	12.32 [e]				(5.35 ± 0.38) × 10^6
	(11.84)				(1.78 × 10^6)
H_2O	15.74				(2.17 ± 0.05) × 10^9
	(16.04)				

[a] pK_{AH}-values taken from ref. 4. [b] Statistically corrected values in parentheses. [c] Four runs carried out within each concentration range. [d] First-order rate constant. [e] Calculated from k_{BOH} = (2.27 ± 0.18) × 10^5.

applicability for OH^- acting as the general base because water is little more acidic than ethanol, but the same mechanism has been proposed recently by Nunez *et al.*[17] for the reverse reaction of similar compounds, the intramolecular addition of alcohol to phthalimide: the point for catalysis by OH^- fell on the Brönsted plot. This work, particularly the value of β_{nuc}, suggests a late transition state for the breakdown step, where proton transfer from water can become favourable. The best evidence in our system is the magnitude of the solvent kinetic isotope effect, which is in the region of two for the reactions of **3**-MUE and **3**-PUE, but inverse for the less highly methylated systems (Table 6).

We can estimate the SKIE for alkaline hydrolysis in the case of compounds **3** as follows, using the fractionation factors

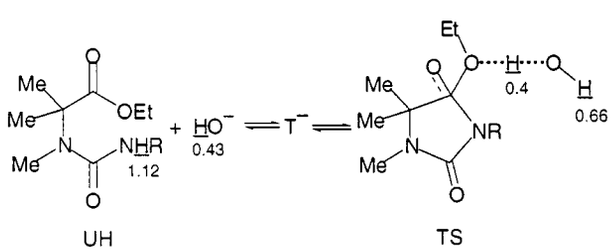

Scheme 4

shown in Scheme 4.[18] (Ground state fractionation factors are from Quinn and Sutton:[19] 0.4 is the usual value for the primary

Table 6 Kinetic solvent isotope effects for the hydroxide ion catalysed cyclization of substituted ethyl hydantoates at 25 °C and ionic strength 1.0 M (KCl)

Compound	pH range (H_2O)	k_{OH}/k_{OD}	Compound	pH range (H_2O)	k_{OH}/k_{OD}
1-MUE	8.8–9.4	0.62 ± 0.06	**1**-PUE	6.0–6.3	0.45 ± 0.04
2-MUE	8.8–9.4	0.74 ± 0.07	**2**-PUE	6.0–6.3	0.67 ± 0.04
3-MUE	8.8–9.4	2.19 ± 0.27	**3**-PUE	6.0–6.3	1.79 ± 0.12

Table 7 Ratios of cyclization rate coefficients for ethyl hydantoates carrying different numbers of methyl groups

Rate ratio	k_H	k_w	k_{AcO^-}	k_{OH^-}	k_{U^-} [a]
2/1-MUE	35			11	46
3/1-MUE	2700			28	36
3/2-MUE	75	40	36	2.4	0.78
2/1-PUE	30			11	35
3/1-PUE	1200			2.6	2
3/2-PUE	39	1.14	1.9	0.23	0.057

[a] Rate constants for cyclization of the ureide anion are given in Table 8.

Table 8 Rates of cyclization of ureide anions U^-

Compound	pK_{NH} [a]	k_{U^-}/s^{-1} [b]
1-MUE	18.8	2.8×10^6
2-MUE	19.45	1.3×10^8
3-MUE	19.0	1.0×10^8
1-PUE	16.0	1.1×10^7
2-PUE	(16.6) [c]	3.8×10^8
3-PUE	(16.0) [d]	2.12×10^7

[a] Data from ref. 8. [b] According to our conclusions about rate-determining step (see text) this rate constant corresponds to k_2 of Scheme 3 for **1**–**2**-MUE and PUE, but to k_3k_2/k_{-2} for **3**-MUE and PUE. [c] Estimated, assuming that the difference between (**1**–**3**)-PUE is the same as for (**1**–**3**)-MUE. [d] Estimated by assuming that the difference in pK is the same in 1 : 1 as in 5 : 1 water : acetonitrile.

isotope effect (the proton in flight) and 0.66 is the secondary effect calculated assuming $a = 0.5$ [eqn. (6)]).

$$\varphi^* = \varphi_R^{1-a}\varphi_P^a = 1^{0.5} \times 0.43^{0.5} = 0.66 \quad (6)$$

The observed SKIE of 1.79 ± 0.12 and 2.19 ± 0.27 (Table 6) for the reactions of **3**-PUE and **3**-MUE, respectively are matched (calculated values $k_H/k_D = 1.82$ and 2.17) using α-values for the specific base-general acid-catalysed process of 0.5 and 0.7. These values indicate a relatively late transition state for the leaving of the ethoxy group.

Since the change in rate-determining step which results in the breakdown of T^- becoming slower than its reversion to products ($k_3 < k_{-2}$ in Scheme 3) is accompanied by slower rates of cyclization for compounds **3** (Table 8), it must involve a slower k_3 step (rather than faster k_{-2}). We suggest that this is a result of steric hindrance to the proton transfer process. The leaving ethoxy groups of **3**-MUE and **3**-PUE are in very crowded environments: the ethyl chain will adopt the least hindered conformation (Fig. 7), blocking the easy access of solvating water molecules. Thus in the half-chair conformation of the presumed transition state of the **3**-MUE reaction the lone pairs are shielded by the methyl groups on C(5) and N(2), and with **3**-PUE screening by the *N*-phenyl group is more effective still (Fig. 7). Where one or both of the C(5) methyl groups is absent this comprehensive shielding disappears.

Although proton transfers between N and O atoms are not generally sensitive to steric effects[20] these have been invoked to explain the slow rates of proton removal from the open form of

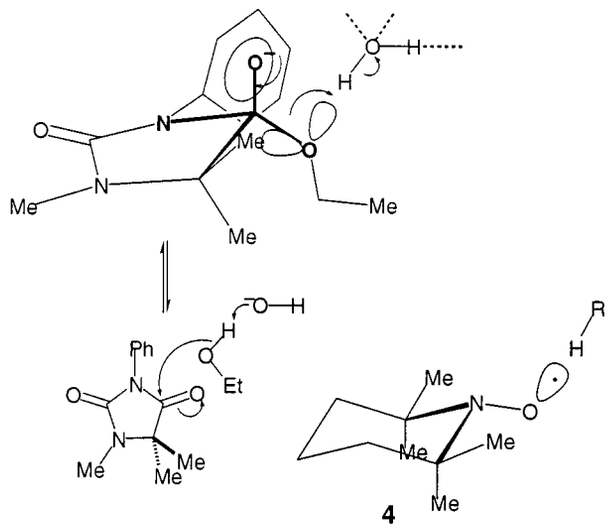

Fig. 7 Steric hindrance of proton transfer to T^- for **3**-PUE: compared with H-abstraction by a hindered aminoxyl radical (**4**).

protonated 1,8-bis(dialkylamino)naphthalenes by hydroxide ion[21] and the protonation of 2,6-di-*tert*-butylpyridine by H_3O^+;[22] as well as (in a less severely hindered situation) the slower rate of exchange of the 3′-NH of biotin.[23] General acid catalysis of acetal hydrolysis is also known to be subject to substantial steric hindrance in hindered systems.[24] Steric hindrance in the case of **3**-T^- is comparable with that in aminoxyl radicals such as **4**, which are protected by the adjacent methyl substituents (as well as stabilized electronically) to such an extent that they do not readily abstract hydrogen atoms from carbon.[25]

It seems unlikely that this factor alone can account for the reversal of the *gem*-dimethyl effect for the cyclization of the anion of $\mathbf{3}^-$, because k_3 is some way from being rate determining for compounds **2**, yet clearly rate-determining for compounds **3**. So though a reduction of an order of magnitude or so could explain the change in rate-determining step, a reduction of several hundred-fold in k_3 is needed to overcome the expected accelerating effect (about 40 according to the data in Table 7) of the additional methyl group. The most likely additional factor is a reduced increase in the equilibrium constant for the formation of the tetrahedral intermediate T. The two adjacent quaternary centres in the five-membered ring (Fig. 7) induce eclipsing interactions between the exocyclic bonds which are absent in the ground state and the product, and most significant for compounds **3**. This effect can explain the smaller kinetic than thermodynamic effective molarities for cyclization reactions of carboxylic acid derivatives: the disparity increases significantly for systems with *gem*-dimethyl groups in the α-position.[26]

For both explanations a key question is why the same factors do not show up in the acid-catalysed cyclization, where the addition of the last methyl in **3** causes accelerations in k_H comparable to addition of the penultimate methyl to give **2** (Table 7). In acid the leaving group in the cyclization reaction is EtOH (from the prototropically-equilibrated intermediate T^+, with a proton on the ethoxy oxygen), and C–O cleavage is not rate determining. The eclipsing interactions in the tetrahedral

intermediate will be similarly unfavourable for both reactions, but less-developed, and thus smaller, in the transition state for C–N bond formation (rate determining in the acid-catalysed reaction). In the reactions of **3** the C–N bond is fully formed in the rate-determining transition state (Fig. 7).

General base catalysis

The cyclization reactions of the six compounds studied in this work are subject to both general acid and general base catalysis, and data for both reactions are shown in the Tables. The disappearance of the *gem*-dimethyl effect is a property specifically of the base-catalysed reaction, so we discuss here only general base catalysis.

The appearance of GBC shows that a process involving rate-determining proton transfer competes with the specific base-catalysed reaction at lower pH. There are only two proton transfers involved in the cyclization reactions of MUE and PUE, the deprotonation of the nucleophilic N and the protonation of the leaving ethoxide anion. General acid catalysis of the departure of ethoxide (kinetically equivalent to GBC) is certainly to be expected, since we have concluded that partial proton transfer from solvent water (see Fig. 7 above) accounts for the solvent kinetic isotope effect observed in the specific base-catalysed cyclization of compounds **3**. However, GAC of this step will make the formation of the tetrahedral intermediate *less* likely to be the slow step of the reaction, so it is not expected to be observed unless it is securely rate determining. We conclude below that the deprotonation of the nucleophilic nitrogen is the step which shows general base catalysis in the general case.

The clearest experimental evidence comes from the Brönsted β-values observed for GBC. These fall into two well-defined categories: *ca*. 0.2 for **2** and **3**-MUE and *ca.* 0.6 for **2** and **3**-PUE. This indicates that no change of mechanism takes place between compounds **2** and **3**: the significant difference appears between the 5-*N*-Me and 5-*N*-Ph esters.

A β-value of 0.6 for PUE is consistent with a rate-determining transition state corresponding to the transition state TS of Scheme 4, with a stronger general acid replacing H_2O. The observed β-value corresponds to $(1 - \alpha)$ for SB/GAC, and the changes in the magnitude of the SKIE for **3**-MUE *vs.* **3**-PUE, which are reproduced by α-values of 0.7 and 0.5, as discussed above, are consistent with the direction of changes of the β-values.

However, two arguments support the involvement of deprotonation of the ureido group in the rate-determining transition state for the cyclizations of the MUE series. The rates for deprotonation by the general base can be calculated from the measured pK-values[8] and the value of k_d, the diffusion controlled rate constant, taken as 10^{10} dm^3 mol^{-1} s^{-1} [eqn. (7)]:

$$k_1 = \frac{K_{NH}}{K_{HA}} k_d \qquad (7)$$

In the case of **2** and **3**-MUE the rate constants estimated for deprotonation by bases weaker than the phosphate dianion are smaller than the rate constants actually observed for catalysis of the cyclization reaction. This means that for **2** and **3**-MUE at least catalysis by the general bases by-passes the high energy ureide anion at low pH.

The second argument is based on reactivity–selectivity relationships, which can make it possible to distinguish between kinetically equivalent mechanisms. A More O'Ferrall–Jencks diagram (see below) accommodates the changes in the β coefficients for deprotonation of the ureido group, but not for proton transfer to the leaving group.

The Brönsted β coefficient of 0.2 observed for the reactions of **2** and **3**-MUE is characteristic of a preassociation mechanism involving hydrogen bond formation (Scheme 5).[27]

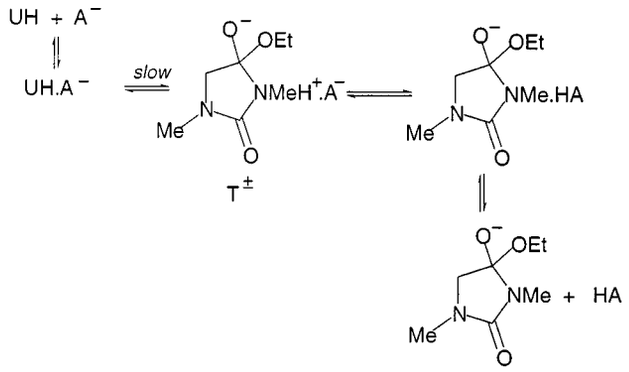

Scheme 5

We suggest that this is the mechanism observed when the lifetime of the intermediate $T^{\pm}$ is shorter than the time for diffusion apart of $T^{\pm}$ and A^-. (A negative deviation from the Brönsted line for general base catalysis is often observed for the water points: this may reflect the favourable electrostatic interaction between the other, anionic, bases and the positively charged nitrogen atom.[28])

In the case of the ω-phenyl derivatives **2** and **3**-PUE the Brönsted β-value of *ca.* 0.6 indicates that proton transfer is well under way in the rate-determining transition state. The simplest mechanism, involving general acid catalysis of the breakdown of T^- (*cf.* Fig. 7, above), can be ruled out with some confidence because the rate constants k_B for general base catalysis are higher for **3**-PUE, in contrast to the hydroxide-catalysed reaction. We conclude that the lifetime of $T^{\pm}$ has reached the point where a concerted mechanism is enforced,[29] because phenylureido is a better leaving group compared to methylureido. The process is illustrated by the alternative route diagram of

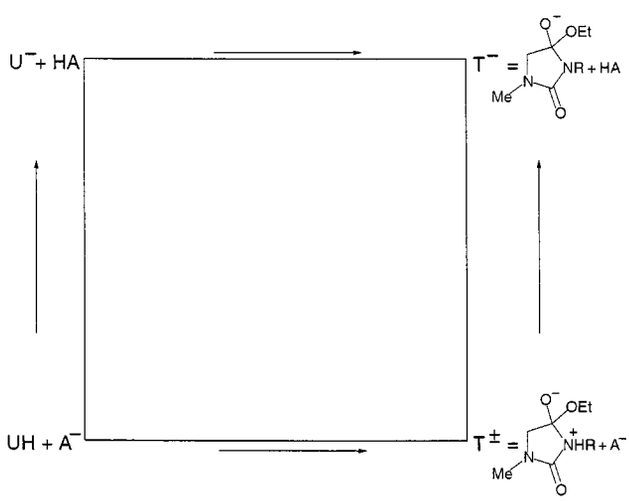

Scheme 6

Scheme 6.[30] Changing R = Me for Ph raises the energy of $T^{\pm}$ and lowers that of U^-, causing a 'perpendicular' shift of the transition state from the bottom right-hand corner towards the centre of the diagram.

Note that a concerted mechanism is not possible from the ground state conformation **5**, which would require the ester carbonyl and the general base to approach the reacting NH simultaneously from the same direction. In the reactive conformation **6**[9] the terminal nitrogen must have rotated out of plane (and conjugation) to allow it to act as a nucleophile in the plane of the incipient five-membered ring, which also makes the reacting NH available to a general base (Scheme 7). The general base is necessary for the less nucleophilic aniline N (R = Ph) but not for R = Me.

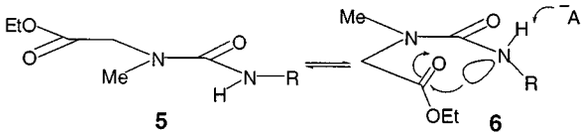

Scheme 7

Structure, conformation and reactivity

1 and **2**-PUE react 2000 times faster than **1** and **2**-MUE in the hydroxide-catalysed reaction, k_{OH}, but are 7 times less reactive in acid (k_H, Table 1). Reactivity in the specific hydroxide-catalysed cyclizations is governed by the p*K*s of the NH protons, which are *ca.* 3 p*K* units lower for the *N*-phenyl compounds, modulated by the *gem*-dimethyl effect.

The rate constants for cyclization of the anions U^- show little sensitivity to electronic effects (3–4 times larger for **1** and **2**-PUE than for **1** and **2**-MUE) but are subject to the *gem*-dimethyl effect. The greater part of the barrier to these very fast reactions probably consists in adopting the proper reactive conformation **6**, as discussed previously.[9] For the anions U^- the reactive conformation about the terminal CO–N bond is obtained directly upon deprotonation from the preferred *Z*-conformation (Scheme 8). On the other hand, of the two substituents on the central N, the bulkier one carrying the ester group will prefer the *Z* conformation and reaction can take place only after rotation to the *E* conformation.

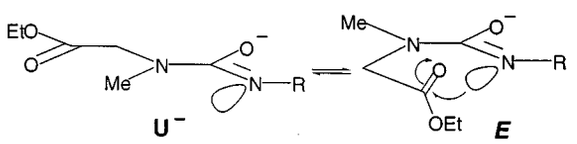

Scheme 8

Thus for the main population of molecules in the ground state the rotational barrier around the C–N partial double bond has to be overcome. The rate constants (k_{U^-}) are of the order of 10^8 s^{-1}, corresponding to a free energy of activation of 6.6 kcal mol^{-1} at 300 K: the conformational barriers in the anions are likely to be of the same order of magnitude (smaller than in the urea because of cross conjugation with the outer CO–N^-). Importantly these barriers decrease upon substitution because of release of ground state strain in the transition state for the formation of **6**: barriers of 11.2 kcal mol^{-1} and 6.3 kcal mol^{-1} have been reported for urea and tetramethylurea, respectively.[31]

The low sensitivity to electronic effects can be attributed to the high reactivity of the anions, thus a simple manifestation of the reactivity–selectivity principle.

Acknowledgements

We thank Professors Andrew Williams, Frank Hibbert and Michael Page for useful discussions, the National Foundation for Scientific Research of Bulgaria for funding this research and the Royal Society of Chemistry for a Journals Grant for International Authors (to I. G. P.).

References

1 J. R. Knowles, *Ann. R. Biochem.*, 1989, **58**, 195.
2 I. B. Blagoeva, I. G. Pojarlieff and A. J. Kirby, *J. Chem. Soc., Perkin Trans. 2*, 1984, 745.
3 H. Slebocka-Tilk, A. J. Bennet, J. W. Keillor, R. S. Brown, J. Peter Guthrie and A. Jodhan, *J. Am. Chem. Soc.*, 1990, **112**, 8507.
4 I. B. Blagoeva, *J. Chem. Soc., Perkin Trans. 2*, 1987, 127.
5 I. B. Blagoeva and I. G. Pojarlieff, *CR. Acad. Bulg. Sci.*, 1977, **30**, 1043; M. Bergon and J.-P. Calmon, *J. Chem. Soc., Perkin Trans. 2*, 1978, 493.
6 A. H. Koedjikov, I. B. Blagoeva, I. G. Pojarlieff and A. J. Kirby, *J. Chem. Soc., Perkin Trans. 2*, 1996, 2479.
7 I. B. Blagoeva, D. T. Tashev and A. J. Kirby, *J. Chem. Soc., Perkin Trans. 1*, 1989, 1157.
8 I. G. Pojarlieff, I. B. Blagoeva, A. J. Kirby, B. P. Mikhova and E. Atay, *J. Chem. Res. (S)*, 1997, 220.
9 I. B. Blagoeva, I. G. Pojarlieff, D. T. Tashev and A. J. Kirby, *J. Chem. Soc., Perkin Trans. 2*, 1989, 347.
10 H. Biltz and K. Slotta, *J. Prakt. Chem.*, 1926, **113**, 233.
11 L. Cuneo, *Ber.*, 1892, **25**, 328.
12 E. Friedman, *Beitr. Chem. Physiol. Pathol.*, 1906, **11**, 184.
13 A. K. Covington, R. A. Robinson and R. G. Bates, *J. Phys. Chem.*, 1966, **70**, 3820; J. C. Fishbein and W. P. Jencks, *J. Am. Chem. Soc.*, 1988, **110**, 5075.
14 J. Kavalek, V. Machacek, G. Svobodova and V. Sterba, *Collect. Czech. Chem. Commun.*, 1986, 51, 375.
15 I. B. Blagoeva, I. G. Pojarlieff and V. Dimitrov, *J. Chem. Soc., Perkin Trans. 2*, 1978, 887.
16 N. Gravitz and W. P. Jencks, *J. Am. Chem. Soc.*, 1974, **96**, 489.
17 O. Nunez, J. Rodrigues and L. Angulo, *J. Phys. Org. Chem.*, 1993, **7**, 80.
18 R. L. Schowen, *Prog. Phys. Org. Chem.*, 1972, **9**, 275; K. B. J. Schowen in *Transition States of Biochemical Processes*, eds. R. D. Gandour and R. L. Schowen, Plenum Press, New York, 1978, p. 225.
19 D. M. Quinn and L. D. Sutton in *Enzyme Mechanism from Isotope Effects*, ed. P. F. Cook, CRC Press, Boca Raton, 1991; quoted from ref. 16, p. 257.
20 F. Hibbert, *Adv. Phys. Org. Chem.*, 1986, **22**, 113.
21 A. Awwal and F. Hibbert, *J. Chem. Soc., Perkin Trans. 2*, 1977, 1589; F. Hibbert and K. P. P. Hunte, *J. Chem. Soc., Perkin Trans. 2*, 1983, 1895.
22 C. F. Bernasconi and D. J. Carre, *J. Am. Chem. Soc.*, 1979, **101**, 2707.
23 C. L. Perrin and T. J. Dwyer, *J. Am. Chem. Soc.*, 1987, **109**, 5163.
24 E. Anderson and T. H. Fife, *J. Am. Chem. Soc.*, 1971, **93**, 1701.
25 L. R. Mahoney, G. D. Mendenhall and K. U. Ingold, *J. Am. Chem. Soc.*, 1973, **95**, 8610.
26 A. J. Kirby, *Adv. Phys. Org. Chem.*, 1980, **17**, 183.
27 M. I. Page and A. Williams, *Organic & Bio-organic Mechanisms*, Longman, London, 1997, p. 178.
28 H. Fischer, F. X. DeCandis, S. D. Ogden and W. P. Jencks, *J. Am. Chem. Soc.*, 1980, 102, 1340.
29 W. P. Jencks, *Chem. Rev.*, 1972, **72**, 702.
30 R. A. More O'Ferrall, *J. Chem. Soc.*, B, 1970, 274.
31 M. Oki, *Applications of Dynamic NMR Spectroscopy to Organic Chemistry*, *Methods in Stereochemical Analysis*, vol. 4, VCH Publishers, Florida, 1985, p. 55.

Paper 8/02884B